Antigen handling and cross-presentation by dendritic cells

Ho, N.I.S.C.

4

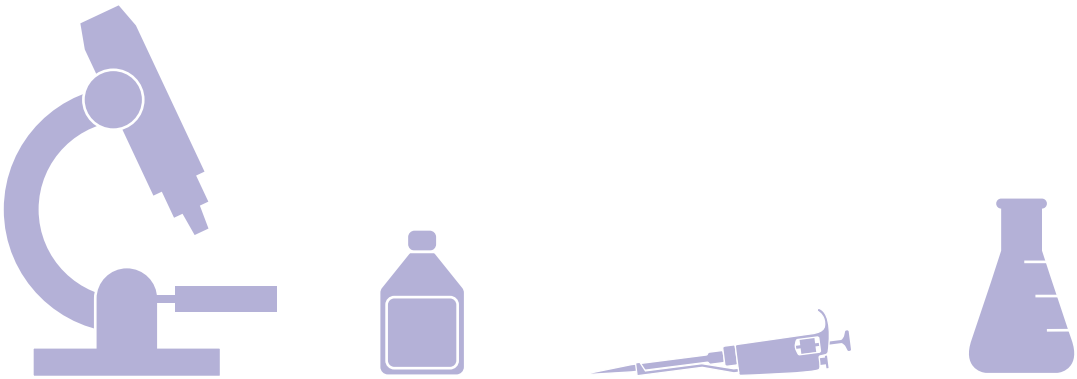

Characterization of antigen-containing compartments after Fcγ receptor or C-type lectin receptor-mediated uptake in dendritic cells

Nataschja I. Ho, Marcel G. M. Camps, Juan J. Garcia-Vallejo, Erik Bos, Abraham J. Koster, Martijn Verdoes, Yvette van Kooyk, Ferry Ossendorp

In preparation

ABSTRACT

An exclusive feature of dendritic cells (DCs) is their capacity to present exogenous antigens by MHC class I molecules, called cross-presentation. Here we showed that protein antigen can be conserved in mature DCs for several days in a lysosome-like storage compartment, distinct from MHC class II and early endosomal compartments, as an internal source for the supply of MHC class I ligands. Using two different uptake routes via Fcγ receptors and C-type lectin receptors, we characterized the antigen-containing organelle 48 hours after antigen uptake as a LAMP1$^+$ compartment lacking the early endosomal markers EEA1 and Rab5. The antigen-containing compartments lacked co-expression of molecules involved in MHC class I processing and presentation including TAP, proteasome subunits and cathepsin proteases. The lack of cathepsin S but the elevated presence of active cathepsin X in the storage compartments in time indicate a role of cathepsin X in antigen processing and cross-presentation by DCs. We could further conclude that the two independent receptor-mediated uptake routes resulted in co-localization of antigen in the same lysosome-like compartments after 48 hours. Our data suggest that these antigen-containing compartments in DC can conserve protein antigens from different uptake routes and contribute to long-lasting antigen cross-presentation.

INTRODUCTION

Dendritic cells (DCs) are an important target for the design and improvement of cancer immunotherapeutic vaccines due to their exclusive ability to cross-present tumor antigens to initiate $CD8^+$ T cell response (1–3). DCs scan the peripheral tissue and take up antigens they encounter through receptors, such as Fcγ receptors (FcγRs) and C-type lectin receptors (CLRs). Upon antigen internalization and DC activation, DCs migrate toward the draining lymph node where they can present antigens to T cells. However, the underlying mechanism of DC cross-presentation is not fully unraveled yet. Two main intracellular pathways for antigen cross-presentation in DCs have been proposed: the vacuolar and the cytosolic pathways. Antigen processing through the vacuolar pathway is mainly dependent on antigen degradation in endosomes, probably by proteases such as cathepsin S, but independent of transporter associated with antigen processing (TAP) and the proteasome (4). Thus, antigen processing and loading on MHCI probably occurs in endocytic compartments. In the cytosolic pathway, exogenous antigens in endosomal vesicles are transported in the cell cytosol and degraded by the proteasome. The peptides that are generated by the proteasome are then transported by TAP to the endoplasmic reticulum (ER) where they are loaded on MHCI molecules (5–7). However, it has been reported that some proteasome-generated peptides can be transported back into endocytic compartments where they are trimmed by insulin regulated aminopeptidase (IRAP) and directly loaded on MHCI molecules (8).

We have reported before that antigen can be stored in DCs for several days which facilitates prolonged cytotoxic T-lymphocyte (CTL) cross-priming capacity (9). Sustained antigen cross-presentation may be important since it can take up to a few days for DCs to migrate from the infection site to the lymph nodes to encounter T cells. Moreover, the turnover rate of surface MHCI molecules is shorter compared to MHCII, most MHCI-peptide complexes disappear from the cell surface within 24 hours (9). Therefore, prolonged antigen storage in DCs and sustained supply of newly synthesized MHCI-peptide complexes is beneficial to ensure efficient T-cell cross-priming (10). Here we further characterize the compartments where antigen is stored in DCs by using immunofluorescent staining of several proteins related to the endosomal trafficking and antigen processing pathways. The lack of cathepsin S indicate that cathepsin S is not involved in antigen degradation in these storage compartments. Interestingly, the increased presence of cathepsin X in the storage compartments in time, suggest there might be a distinct but yet unidentified function of cathepsin X in antigen storage or processing in DCs. Moreover, we compared the routing of antigens targeted to FcγRs and C-type lectin receptor MGL1. Our results revealed that antigens targeted to FcγRs or MGL1 end up in the same storage compartment. The storage compartment is characterized as LAMP1 positive, distinct from early endosomal or MCHI/ MHCII loading compartments. Our data suggest that these storage compartments can conserve antigens from different uptake routes which can contribute to long-lasting DC antigen cross-presentation.

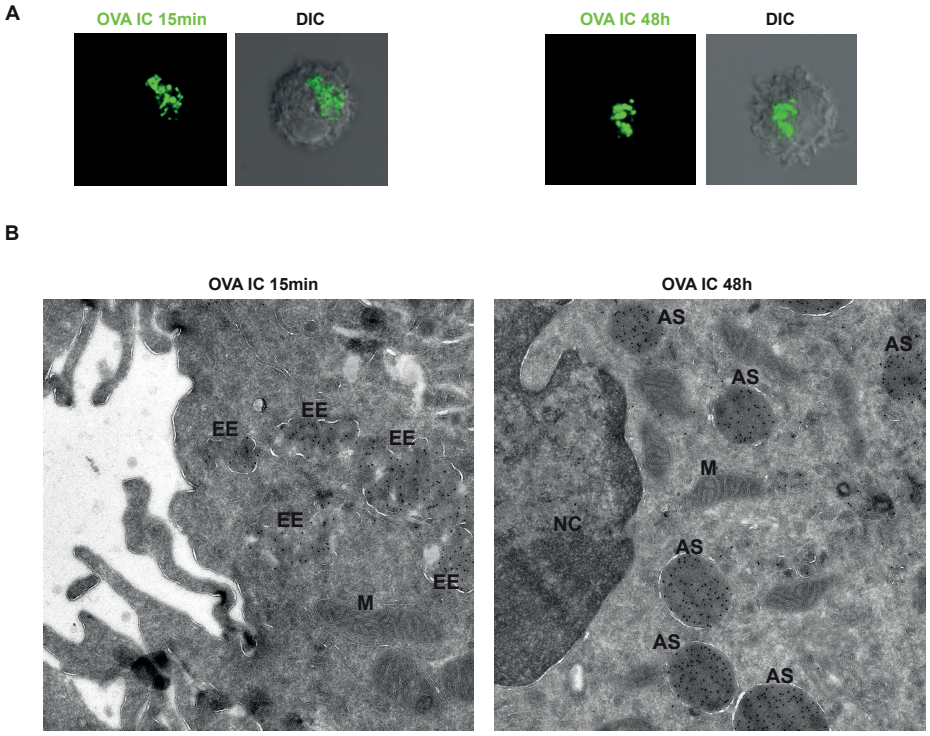

Figure 1. Antigen storage in dendritic cells. DCs were pulsed with OVA IC (Alexa Fluor 488) for 15 min **(A, left panel)** or pulsed with OVA IC for 2 hours and chased for 48 hours **(A, right panel)**. OVA IC uptake and presence in DCs were imaged by confocal microscopy and differential interference contrast (DIC) was additionally used to image cell contrast. Immuno-electron microscopy images of DCs after 15min OVA IC (Alexa Fluor 488) pulse **(B, left)** and DCs pulsed with OVA IC for 2 hours and chased for 48 hours **(B, right)**. Sections were labelled with immunogold for Alexa488 with 10nm gold particle size. EE= early endosome, M= mitochondria, AS= antigen storage compartment, NC= nucleus.

RESULTS

Antigen-antibody complexes are stored in LAMP1 positive compartments in dendritic cells

We have studied the uptake kinetics before of OVA bound to OVA-specific IgG antibodies (OVA immune complexes, OVA IC) and showed that the uptake of OVA IC is a 1000-fold more efficient than soluble OVA (9). Indeed, large amounts of fluorescently labeled OVA IC were already taken up by DCs after only 15 min pulse with OVA IC, visualized by confocal microscopy (Fig. 1A, left panel). Interestingly, DCs that were pulsed with OVA IC for 2 hours, washed, and chased for 48 hours still contain extensive amounts of OVA IC (Fig 1A, right panel). These OVA IC are located perinuclear in a condensed fashion. More detailed visualization of the uptake of OVA IC was done by 10 nm gold particle labeling for electron

microscopy. After 15 min OVA IC pulse in DCs, many gold beads were detected in cloud shaped compartments (Fig. 1B, left). Strikingly, 48 hours after pulse-loading DCs with OVA IC, large spherical structures filled with gold beads were visualized near the nucleus (Fig. 1B, right). These results confirmed once more that antigen can be stored in DCs for several days in compartments proportionate to endosomal structures. Therefore, we performed co-staining with antibodies against several members of the endosomal trafficking pathways to further characterize the storage compartments with confocal microscopy. After the initial 15 min uptake of OVA IC by DCs, OVA IC are taken up in EEA1 and Rab5 positive compartments (Fig. 2, Supplemental Fig. 1). However, after the 48h chase, OVA IC were not found in EEA1 or Rab5 compartments. Rab7, which is a marker for more matured endosomes, did not show any co-localization with OVA IC after 15 min or 48 hours. The lysosomal marker LAMP1 was spread out through the cell cytosol after 15 min and no co-localization was found with OVA IC. However, a clear perinuclear reorganization of LAMP1 was detected after 48 hours and co-localization with OVA IC was observed. MHCI and MHCII positive compartments in the cell cytosol were detected at 15 min time point, and co-localization with OVA IC was observed (Fig. 2, Supplemental Fig. 1). As described before, targeting FcγRs on DCs with OVA IC induced strong DC maturation, including an increased expression of MHCI and MHCII (9). Indeed, 48 hours after antigen pulse, most MHCI and MHCII were detected on the cell surface, and not co-localizing anymore with OVA IC (Fig. 2, Supplemental Fig. 1). Since we have shown before that antigens from the storage compartments are cross-presented in a TAP and proteasome dependent pathway (9), antibody staining for TAP1 and PA28β was performed. The proteasome activator PA28b subunit is known to be strongly upregulated in maturing dendritic cells (11). However, neither TAP1 nor PA28β co-localized with OVA IC at any measured time point (Fig. 2, Supplemental Fig. 1).

In order to follow the co-localization kinetics of OVA IC after uptake by DCs, we used imaging flow cytometry, a method that allows high-throughput image analysis of cells in flow with near-confocal resolution to analyze intracellular routing of fluorescently labeled OVA IC. OVA IC enters EEA1 positive compartments after DC uptake but the co-localization score decreased swiftly within 15 min (Fig. 3). One hour after the initial antigen pulse, most OVA IC were not present in EEA1 positive compartments. Similar kinetics were observed for Rab5, OVA IC enters Rab5 positive compartments, but after 1 hour, the co-localization score between Rab5 and OVA IC had diminished. In line with the confocal analysis, Rab7 did not show any remarkable co-localization with OVA IC, although a slight increase could be observed after 48 hours. OVA IC was strongly co-localizing with LAMP1 after 24 and 48 hours, confirming our previous confocal data. MHCI and MHCII co-localized with OVA IC at early time points (10 min, 1 hour) but the co-localization score was decreased after 24 and 48 hours. The co-localization kinetics for both TAP1 and PA28β with OVA IC did not change in time.

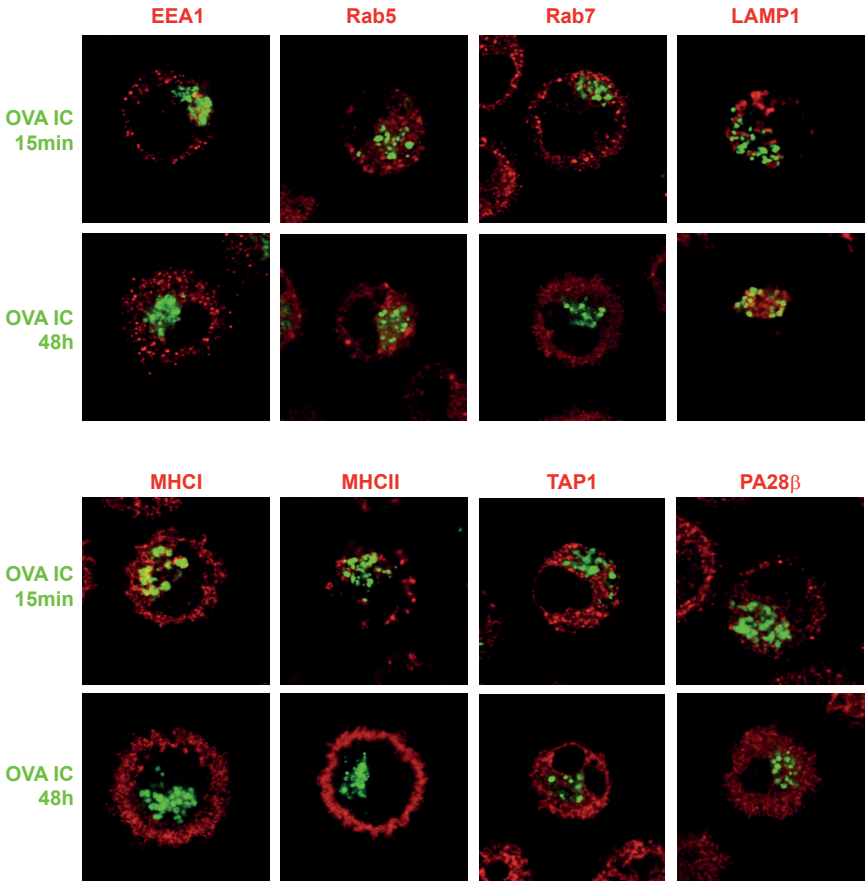

Co-localization	EEA1	Rab5	Rab7	LAMP1	MHCI	MHCII	TAP1	PA28β
OVA IC 15min	+	+	-	-	+	+	-	-
OVA IC 48h	-	-	-	+	-	-	-	-

Figure 2. Characterization of the antigen storage compartments in DCs upon FcγR targeting. DCs were pulsed with OVA IC (Alexa Fluor 488, green) for 15 min or pulsed with OVA IC for 2 hours and chased for 48 hours. OVA IC presence in DCs was imaged by confocal microscopy and DIC was used to image cell contrast. Specific antibodies against EEA1, Rab5, Rab7, LAMP1, MHCI, MHCII, TAP1, and PA28β (red) were used and analyzed for co-localization with OVA IC. Co-localization between OVA IC and the antibodies is summarized in a table, "+" indicates co-localization, "-" indicates no co-localization.

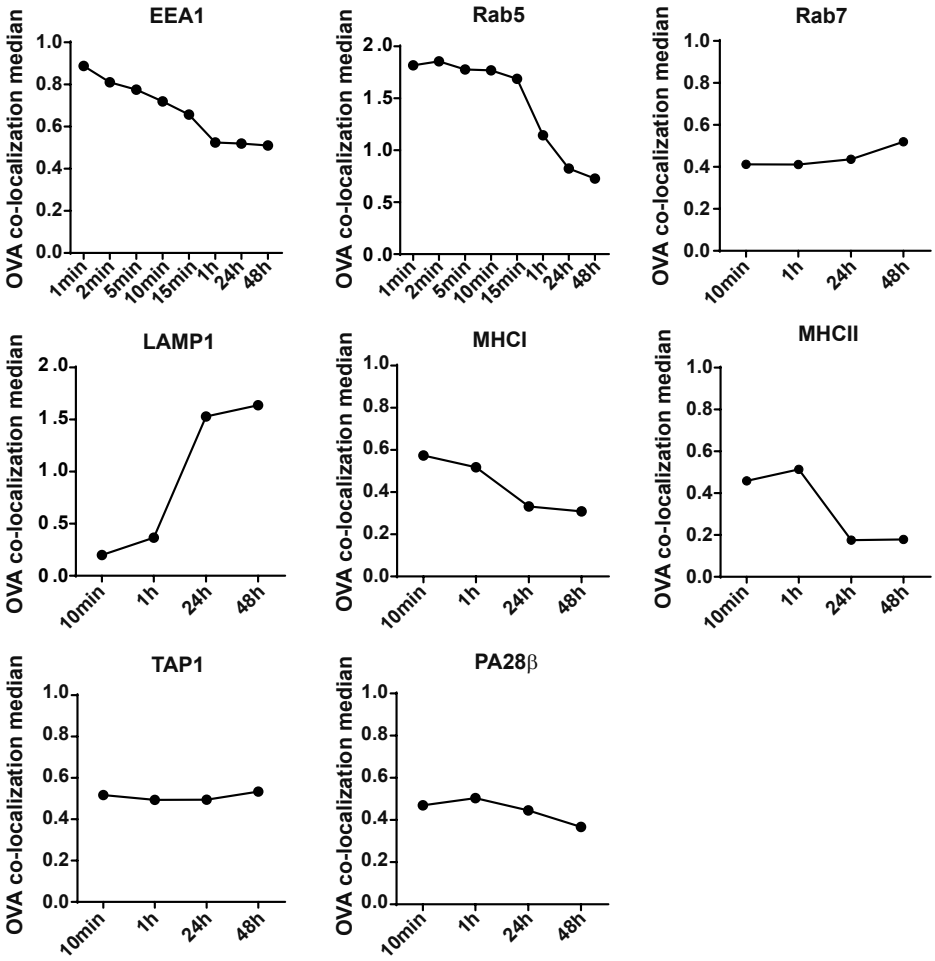

Figure 3. Characterization of the antigen storage compartments in DCs with imaging flow cytometry. DCs were pulsed with OVA IC (Alexa Fluor 647 labeled OVA) for 1, 2, 5, 10, 15 min, or 1 hour (different for each antibody), and pulsed for 2 hours and chased for 24 and 48 hours. Co-localization between OVA IC and EEA1, Rab5, Rab7, LAMP1, MHCI, MHCII, TAP1, and PA28β was analyzed by imaging flow cytometry.

Taken together, we observed that OVA IC enter the early endosomal pathway after uptake by DCs. Besides, OVA IC are present in endosomal compartments that contain MHCI and MHCII at early time points. However, at later time points (24 and 48 hours), OVA IC are stored in LAMP1 positive compartments, distinct from early endosomal and MHCII loading compartments. Since TAP1 and PA28β were not detected in the antigen storage compartments, but shown before to be crucial in antigen processing and cross-presentation (11, 9), this suggests that antigen is translocated from the storage compartments into the cell cytosol for further processing.

Antigen storage compartments contain cathepsin X but no cathepsin S

Since antigen storage compartments can be characterized as lysosomal-like compartments, we investigated the role of lysosomal proteases, such as cysteine cathepsins. The role of cathepsin S in antigen degradation have been described for the vacuolar pathway in DC cross-presentation (4). Whether cysteine cathepsins play a role in endosome-to-cytosol pathway is not excluded. Therefore we investigated the presence of proteolytically active cysteine cathepsins in antigen storage compartments in DCs with the use of the cysteine cathepsin quenched activity-based probe (qABP) BMV109 (12). This intrinsically dark qABP reacts with active cathepsin X, B, S, and L to yield a fluorescent Cy5 conjugate. Lysates of naïve DCs exposed to 1 μM BMV109 for 1 hour were run on 15% PAGE gel and scanned for Cy5 fluorescence to show the presence of active cathepsin X, B, S, and L, with cathepsin S being the most dominantly labeled (Fig. 4A, left lane). Interestingly, after 2 hours OVA IC pulse and 24 hours chase, the amount of cathepsin X was increased compared to immature DCs (Fig. 4A, right lane). We continued to investigate cathepsin S and X with the use of confocal microscopy to analyze their presence in the antigen storage compartments. BMV109 labeling showed partial co-localization with antibody-stained cathepsin S in naïve DCs (Fig. 4B, Supplemental Fig. 2A). DCs that were pulsed with fluorescently labeled OVA IC for 30 min revealed co-localization of OVA IC with BMV109 labeling, but not with cathepsin S (Fig. 4B, Fig. 4D, Supplemental Fig. 2B). After 2 hours OVA IC pulse and 24 hours chase, co-localization between OVA IC and BMV109 labeling was more distinct, but no co-localization was observed with cathepsin S (Fig. 4B, Fig. 4D, Supplemental Fig. 2B). A more detailed kinetic experiment following co-localization of OVA IC with cysteine cathepsin activity and cathepsin X in time revealed that BMV109 labeling and cathepsin X were distributed in the cell cytosol in naïve DCs, but became more clustered to a central location 3 hours after OVA IC uptake (Fig. 4C, Supplemental Fig. 2C). Moreover, after 30 min, one hour, or 2 hours OVA IC pulse, OVA IC were co-localizing with BMV109 fluorescence but not with cathepsin X (Fig. 4C, Fig. 4D, Supplemental Fig. 2D). After 3 hours OVA IC pulse, co-localization between OVA IC and BMV109 labeling, and partial co-localization between OVA IC with cathepsin X was observed. When DCs were pulse-loaded with OVA IC for 2 hours and chased for 24 hours, both the BMV109 fluorescence and cathepsin X were co-localizing with OVA IC (Fig. 4C, Fig. 4D, Supplemental Fig. 2D). These results indicate that the antigen storage compartments in DCs contain cathepsin X and possibly other yet unidentified cathepsins, such as cathepsins B or L.

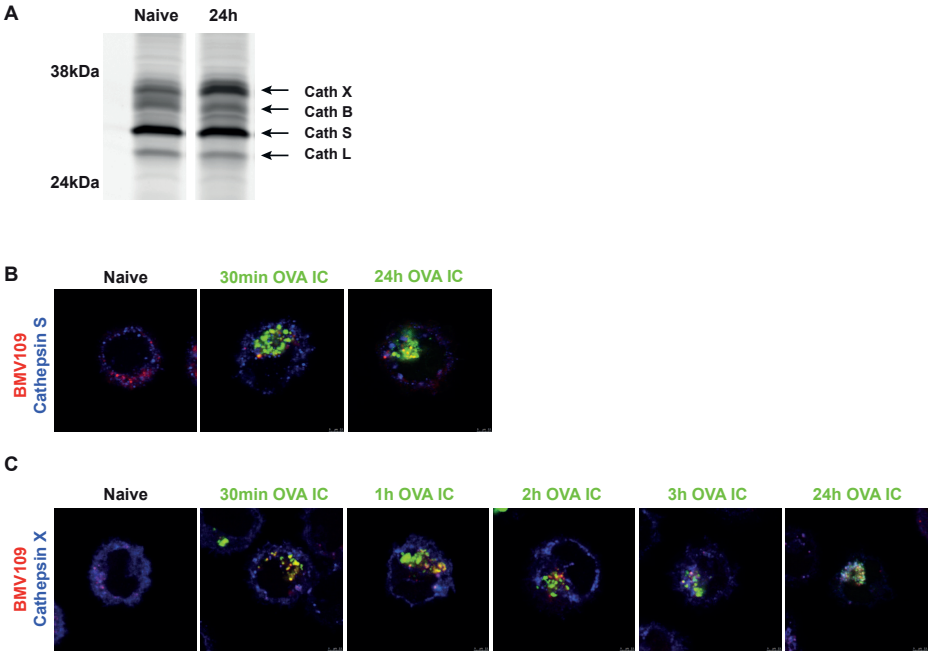

D

Co-localization	BMV109	Cathepsin X	Cathepsin S
OVA IC 30min	+	-	-
OVA IC 1h	+	-	n/a
OVA IC 2h	+	-	n/a
OVA IC 3h	+	+/-	n/a
OVA IC 24h	+	+	-

Figure 4. The presence of cathepsins in the antigen storage compartments in DCs. Naïve DCs or DCs pulsed with OVA IC for 2 hours and chased for 24 hours were run on a 15% PAGE gel. Quenched activity-based probe BMV109 was used to stain active cathepsin X, B, S, and L, indicated by arrows **(A)**. Co-localization between BMV109 (red) and specific antibody against cathepsin S (blue) was analyzed in naïve DCs with confocal microscopy. DCs were pulsed with OVA IC (Alexa Fluor 488) for 30 min or pulsed for 2 hours and chased for 24 hours. Co-localization between OVA IC (green), cathepsin S (blue), and BMV109 (red) was analyzed by confocal microscopy **(B)**. Naïve DCs, DCs pulsed with OVA IC (Alexa Fluor 488) for 30 min, 1, 2, 3 hours or DCs pulsed for 2 hours and chased for 24 hours were stained with cathepsin X antibody and BMV109. Co-localization between OVA IC (green), cathepsin X (blue), and BMV109 (red) was analyzed by confocal microscopy **(C)**. Co-localization between OVA IC, BMV109, cathepsin X, and cathepsin S is summarized in a table, "+" indicates co-localization, "+/-" indicates partial co-localization, "-" indicates no co-localization, "n/a" indicates not applicable **(D)**.

Antigen uptake by FcγRs and MGL1 routes the antigen to the same storage compartments

To investigate whether the fate of antigen taken up by a different DC uptake receptor is similar to antigen taken up by FcγRs, we investigated antigen targeting via the C-type lectin receptor MGL1. We have described before that modification of OVA with the glycan-structure

Lewis^X (Le^X) re-directs OVA to MGL1 and induce enhanced T cell cross-priming (13). Here we pulsed DCs with fluorescently labeled OVA IC and OVA-Le^X and followed the antigen in time. Fifteen minutes after antigen pulse, great amounts of both OVA IC and OVA-Le^X were already taken up by DCs (Fig. 5A, Supplemental Fig. 3). Punctuated hotspots of OVA IC and OVA-Le^X were spread through the cell cytosol and showed partial co-localization. After one hour, OVA IC and OVA-Le^X were more compactly distributed in the cell cytosol compared to 15 minutes, still showing partial co-localization (Fig. 5A, Supplemental Fig. 3). More strikingly, after 2 hours pulse loading DCs and 24 hours or 48 hours chase, both OVA IC and OVA-Le^X appeared as concentrated hotspots near the nucleus of DCs (Fig. 5A, Supplemental Fig. 3). Co-localization analysis showed complete overlap of both OVA IC and OVA-Le^X indicating the antigens were present in the same compartments (Supplemental Fig. 3). These results demonstrate that targeting antigen to DCs through FcγRs and MGL1 routes the antigen to the same storage compartments at later time points.

Antigen targeted to MGL1 is stored in LAMP1 positive compartments in DCs

Our previous results suggest that antigen taken up via MGL1 by DCs end up in the same compartments as antigen targeted to FcγRs. To further characterize the routing, DCs were pulsed with fluorescently labeled OVA-Le^X for 15 min or pulsed for 2 hours and chased for 48 hours. Co-staining between OVA-Le^X and several members of the endosomal trafficking and processing pathways was performed and analyzed by confocal microscopy. After 15 min pulse, OVA-Le^X was distributed through the cell cytosol and co-localization with EEA1 and partially with Rab5 was observed (Fig. 5B, Supplemental Fig. 4). After 48 hours, OVA-Le^X was redistributed in a more compact manner located near the nucleus and not co-localizing with either EEA1 or Rab5. No co-localization between OVA-Le^X and Rab7 was observed at the measured time points (Fig. 5B, Supplemental Fig. 4). Since we showed that OVA IC and OVA-Le^X co-localized after 24 hours chase, and we observed co-localization of OVA IC with LAMP1 after 48 hours, one could speculate that OVA-Le^X also ends up in similar LAMP1 positive compartments. Indeed, we observed an overlap of OVA-Le^X with LAMP1 after 48 hours, whereas no co-localization was observed after 15 min antigen pulse (Fig. 5B, Supplemental Fig. 4). Interestingly, OVA-Le^X is present in intracellular MHCI and MHCII positive compartments during the early stage of antigen uptake, but after 48 hours chase both MHCI and MHCII were mainly expressed on the cell surface and not co-localizing with OVA-Le^X (Fig. 5B, Supplemental Fig. 4). Both TAP1 and PA28β did not co-localize with OVA-Le^X regardless of the measured time points (Fig. 5B, Supplemental Fig. 4). These results indicate that OVA-Le^X is following a similar uptake routing as FcγR-targeted OVA IC and both end up in the same LAMP1 positive storage compartments.

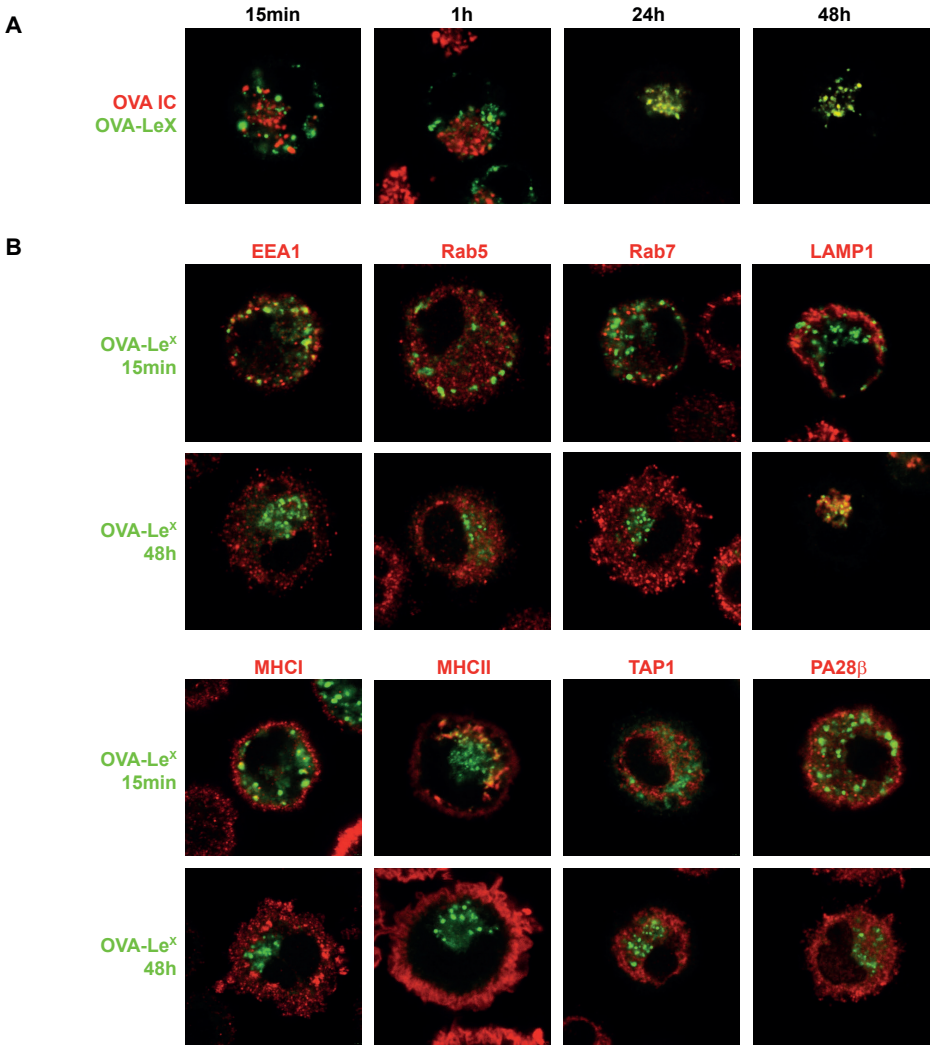

Co-localization	EEA1	Rab5	Rab7	LAMP1	MHCI	MHCII	TAP1	PA28β
OVA-Le^x 15min	+	+	-	-	+	+	-	-
OVA-Le^x 48h	-	-	-	+	-	-	-	-

Figure 5. Antigens targeted to FcγRs and MGL1 on DCs end up in the same compartment. DCs were pulsed with OVA IC (Alexa Fluor 647) or OVA-Le^x (Dylight 488) for 15 min and 1 hour, or pulsed for 2 hours and chased for 24 or 48 hours. Co-localization between OVA IC (red) and OVA-Le^x (green) was visualized by confocal microscopy **(A)**. DCs were pulsed with OVA-Le^x (Dylight 488) for 15 min or pulsed with OVA-Le^x for 2 hours and chased for 48 hours. OVA-Le^x presence in DCs was imaged by confocal microscopy and specific antibodies against EEA1, Rab5, Rab7, LAMP1, MHCI, MHCII, TAP1, and PA28β (red) were used and analyzed for co-localization with OVA-Le^x (green). Co-localization between OVA-Le^x and the antibodies is summarized in a table, "+" indicates co-localization, "-" indicates no co-localization **(B)**.

DISCUSSION

We have previously described that antigen can be stored in dendritic cells (DCs) for several days which is beneficial for prolonged antigen presentation to $CD8^+$ and $CD4^+$ T cells (9). In the current study, we have characterized the storage compartments in DCs by tracking protein antigens targeted to FcγRs and C-type lectin receptor MGL1. Several markers of the endosomal trafficking and antigen processing pathways were investigated for co-localization with fluorescently labeled antibody-bound OVA immune complexes (OVA IC) targeted to FcγRs at different time points and detected by confocal microscopy and imaging flow cytometry. We observed that OVA IC were efficiently taken up by DCs already after 15 min. The antigen first entered early endosomal compartments characterized by the presence of EEA1 and Rab5. Co-localization with MHCI and MHCII was also detected after 15 min OVA IC uptake, suggesting a route for early antigen presentation. However, when DCs were pulse loaded with OVA IC and chased for 48 hours, OVA IC were stored in LAMP1 positive compartments, distinct from EEA1, Rab5 or MHCI/ MHCII loading compartments. Moreover, TAP1 or the proteasomal activator PA28β were not present in the storage compartments. We have shown before that antigen cross-presentation from the storage compartments is TAP1 and proteasome dependent, suggesting that antigen is translocated from the storage compartments into the cytosol for further processing before loading on MHCI (9). It has been reported that in the endosome-to-cytosol pathway antigens need to be transported from endosomal compartments into the cytosol where they are degraded by the proteasome (6, 7). After proteasomal degradation, these derived peptides are further transported by TAP into the ER. However, it has also been reported that some proteasome-generated peptides may be transported back into endocytic compartments and trimmed by IRAP and then directly loaded on MHCI molecules (8).

Lysosomal proteases, such as cathepsin S, are essential for the generation of antigenic peptides for MHCII antigen presentation, Ii degradation and dissociation from MHCII (14, 15). Besides, cathepsin S, B, H, and L redistribute from lysosomes to MHCII-containing endosomal antigen-processing compartments upon DC activation (16). The role of cathepsin S in antigen degradation has been described for the vacuolar pathway in DC cross-presentation (4). Whether cathepsins play a role in endosome-to-cytosol antigen cross-presentation pathway is not reported yet. Here we show that the antigen storage compartments containing OVA IC lack cathepsin S activity, but do possess cathepsin X activity, as determined by qABP (BMV109) labeling of cysteine cathepsin activity in combination with immunofluorescence staining. We observed co-localization of cysteine cathepsin activity with OVA IC already after 30 min uptake. However, staining with antibodies against cathepsin S or cathepsin X did not show any co-localization with OVA IC after 30 min uptake. The storage compartments where

antigen is conserved during later stage were cathepsin S negative but contained cathepsin X, however the presence of other cathepsins could not be ruled out.

Rapid antigen degradation of internalized antigen is assumed to be negatively affecting cross-presentation outcome. It has been demonstrated that DCs expressed lower levels of lysosomal proteases compared to macrophages (17). Expression of cathepsin L, S, D, and B in DC phagosomes was reduced compared to macrophages, which could impair phagolysosomal degradation and sustained antigen stability in DCs. Cathepsin X is predominantly found in monocytes, macrophages, and dendritic cells (18). It has been described that cathepsin X played a role in β2 integrin activation in DCs, which was crucial for affective antigen presentation and initiation of T cell immune response (19). Obermajer *et al.* showed that during DC maturation, cathepsin X translocated to the plasma membrane and enabled Mac-1 activation and cell adhesion (20). Moreover, cathepsin X redistributed from the membrane to the perinuclear region in mature DCs, which coincided with de-adhesion of DCs, cell cluster formation, and acquisition of the mature phenotype. Importantly, they showed that inhibition of cathepsin X in DCs reduced cell surface expression of co-stimulatory molecules, abolished cytokine production, diminished DC migration, and decreased stimulation of $CD4^+$ T cells. However, the role of cathepsin X on DC cross-presentation still needs to be elucidated.

We found similar endosomal trafficking results of fluorescently labeled antigen targeted to the C-type lectin receptor MGL1 compared to FcγRs targeting. The antigen was first present in EEA1/ Rab5 positive early endosomes, containing MHCI and MHCII, but was subsequently stored in LAMP1 positive compartments lacking TAP and PA28β after 48 hours chase. These results indicate that antigen targeted to FcγRs or MGL1 on DCs follows a similar antigen routing pathway, ending up in the same storage compartments. We have published before that MGL1 targeting involved antigen routing to a Rab11/LAMP1 positive compartment and that the cross-presentation is TAP and cathepsin S independent (13). This seems contradictory to our previous results where we showed that antigen cross-presentation after targeting FcγRs is TAP and proteasome dependent (9). However, an important note is that relative early cross-presentation was measured in the MGL1 setting, only 4 hours after antigen pulse, whereas antigen cross-presentation from the storage compartments occurred at later time points, as described for OVA IC targeted to FcγRs after 48 hours chase. Nevertheless, antigen uptake by MGL also induced sustained antigen cross-presentation when measured after 48 hours chase (13). It could be possible that there is a distinction between early and late antigen processing and cross-presentation in DCs. One can speculate that during the early stage after antigen uptake, antigen is processed and loaded on MHCI directly in early endosomes, which is TAP and proteasome independent. In this case, MHCI molecules could be derived from Rab11 positive endosomal recycling compartments (21). However, when antigen stays longer in DCs and resides in LAMP1

positive compartments, which lack direct processing and loading machineries, the antigen needs to be translocated from the storage compartments to the cytosol for proteasomal degradation and subsequently transported via TAP to MHCI loading sites.

Since the turnover rate of surface MHCI molecules is shorter compared to MHCII, most MHCI-peptide complexes disappear from the cell surface within 24 hours (9). The migration of DCs after antigen encountering to the T-cell zones might take up to several days, therefore prolonged antigen storage in DCs and sustained supply of newly synthesized MHCI-peptide complexes is beneficial to ensure efficient T-cell cross-priming (10). The current study was performed with *in vitro* cultured BMDCs, however the existence and relevance of antigen storage compartments *in vivo* was confirmed by our previous work where we showed sustained antigen presence in different DC subsets and prolonged cross-presentation *in vivo* (22). The presence of storage compartments was visible after isolation of both $CD8\alpha^+$ and $CD8\alpha^-$ DC subsets after *in vivo* antigen uptake, showing similar punctuated endosomal structures. These DC subsets could efficiently present antigen to $CD8^+$ and $CD4^+$ T cells, respectively. Taken together, our studies indicate the importance of antigen storage compartments in DCs *in vitro* as well as *in vivo*.

Next to direct antigen uptake, processing, and presentation, also carry-over of antigen from one DC type to another is currently accepted as a feasible model of cross presentation *in vivo* (23–25) as the role of multiple DC subsets in T cell priming become more evident (26–29). In this two-step priming model, naïve $CD4^+$ and $CD8^+$ T cells are activated by different DC populations. The activated $CD8^+$ T cells recruit lymph node-resident $XCR1^+$ DCs which receive cross-presented antigen from the DCs that carried out the first priming step (30, 31). The $XCR1^+$ DCs interact with both activated $CD4^+$ and $CD8^+$ T cells and thereby inducing optimal signals for $CD8^+$ T cell differentiation into cytotoxic T lymphocytes (CTLs) and memory CTLs. We speculate that antigen storage compartments may play a central role in these processes between cell types as well since prolonged antigen storage and presentation by DCs would be beneficial for this multi-step T cell priming model.

Here we show that antigen targeted to different uptake receptors on DCs can result in the same antigen routing and ultimately conserved in LAMP1 positive storage compartments. The absence of core components of the antigen processing and loading machineries in these compartments suggest that the main function of the compartments is to store antigen for sustained antigen presentation, which is crucial to elicit prolonged efficient T cell priming. Furthermore, antigen degradation in the storage compartments could be slower due to the lack of cathepsin S. Additional research is needed to determine the role of cathepsin X in antigen storage and DC cross-presentation. The current understanding of the intracellular pathways underlying DC cross-presentation reveals a complex molecular and subcellular interplay.

MATERIALS AND METHODS

Cells and antigen stimulation

Bone marrow-derived dendritic cells (BMDCs) from C57BL/6 mice were generated in the presence of 30% R1 supernatant from NIH3T3 fibroblasts transfected with GM-CSF for 10 days. OVA-IgG immune complexes (OVA IC) were formed by incubating 1 µg/ml OVA (Alex Fluor 488 or 647 conjugated; Life Technologies) and 300 µg/ml anti-OVA IgG (rabbit polyclonal, LSBio) for 30 min at 37^{0}C. BMDCs were loaded with OVA IC for different time points, as indicated in each experiment. For the pulse-chase experiments, BMDCs were pulsed for 2 hours with OVA IC, washed, and chased for 24 or 48 hours. BMDCs were incubated with 30µg/ml OVA-Le^x (Dylight 488) (kindly gifted by Yvette van Kooyk) for 15 min or pulsed for 2 hours, washed, and chased for 48 hours.

Confocal microscopy

BMDCs were incubated with OVA IC (Alexa Fluor 488, or 647 conjugated) or OVA-Le^x (Dylight 488) for the indicated time points. Cells were washed and transferred to glass bottom dishes (MatTek corporation, Ashland, USA), fixed with 4% formaldehyde (Merck) and permeabilized with 0.5% saponin. Cells were then incubated with one of the following primary antibodies: goat anti-EEA-1 (C-15, Santa Cruz Biotechnology), LAMP-1 (CD107a, Alexa Fluor 647, BioLegend), mouse anti-Rab5 (D11, Santa Cruz Biotechnology), mouse anti-Rab7 (Rab7-117, Sigma-Aldrich), rat anti-MHCI ((H-2D^b, ER-HR 52, Abcam), rat anti-MHCII (I-A/I-E, M5/114.15.2, BioLegend), goat anti-TAP1 (B-8, Santa Cruz Biotechnology), and goat anti-PA28β (L-19, Santa Cruz Biotechnology). The following secondary antibodies were used: goat anti-mouse IgG (H+L) Alexa Fluor 647, rabbit anti-goat IgG (H+L) Alexa Fluor 647, and donkey anti-rat IgG (H+L) Alexa Fluor 647, all from ThermoFisher Scientific. For the cathepsin experiments, BMDCS were incubated with OVA IC (Alexa Fluor 488) for the indicated time points. Cells were fixed and permeabilized as described before and then incubated for 30 min with 1µM cysteine cathepsin activity-based probe BMV109 which was provided by Martijn Verdoes (12). The cathepsin probe covalently reacts with the active site of Cathepsin X, B, S, and L. Once the probe binds to the target enzyme, the quencher is removed and the probe emits the fluorophore Cy5. Co-staining was performed with the following primary antibodies: mouse anti-cathepsin S (E-3, Santa Cruz Biotechnology), and polyclonal goat anti-cathepsin X/Z/P (R&D systems). The following secondary antibodies were used: goat anti-mouse IgG A568 (H+L, ThermoFisher Scientific), and rabbit anti-goat A568 (H+L, ThermoFisher Scientific). The cells were imaged using Leica SP5 STED confocal microscope with a 63x objective lens. Differential interference contrast (DIC) was additionally used to image cell contrast. Images were acquired in 10x magnification and processed with ImageJ software.

Imaging flow cytometry

BMDCs were incubated with OVA IC (Alexa Fluor 647) for the indicated time points, fixed with 4% formaldehyde (Merck) and permeabilized with 0.5% Saponin. Cells were stained with primary antibodies as described under the confocal microscopy section and subsequently stained with the following secondary antibodies: goat anti-mouse IgG $F(ab')_2$ Alexa Fluor 488, donkey anti-rat IgG (H+L) Alexa Fluor 488 (both from ThermoFisher Scientific), and rabbit anti-goat IgG Cy3 (Jackson ImmunoResearch). Cells were acquired on an ImageStream X100 (Amnis) imaging flow cytometer. A minimum of 15000 cells was measured per sample at a flow rate ranging between 50 and 100 cells/sec at 60x magnification, the analysis was performed using the IDEAS v6.1 software (Amnis). Cells were first gated based on the Gradient RMS (brightfield) feature and then further gated based on area vs aspect ratio intensity (both on brightfield). The first gating identified the cells which appeared in focus, while the second gating excluded doublets and other cells than BMDCs. Co-localization between OVA IC and the markers was calculated using the bright detail co-localization feature.

Electron microscopy

BMDCs were incubated with OVA IC (Alexa Fluor 488) for 15 min or 2 hours, washed, and chased for 48 hours. Cells were fixed for 2 hours in PHEM buffer containing 2% paraformaldehyde and 0.2% glutaraldehyde. The cells were rinsed in PBS and pelleted in pre-warmed PBS containing 12% gelatin. The cell pellet was prepared for cryo sectioning and immunogold labelling as described elsewhere (32). Briefly, small blocks were cut form the cold cell pellet, which were infiltrated in 2.3M sucrose in phosphate buffer for 3 hours. The cryo-protected samples were plunged in liquid nitrogen and sectioned with a cryo ultramicrotome (Leica, Vienna) using a diamond knife (Diatome, Biel). Ultra-thin sections (70 nm) were labelled with protein A gold (10 nm, CMC, Utrecht) and embedded in 2% methylcellulose in water containing 0.6% uranyl acetate and subsequently air-dried. The sections were imaged in a Tecnai 12 transmission electron microscope (Thermo Fisher) operating at 120kV equipped with a 4K Eagle camera (Thermo Fisher).

Fluorescent SDS-PAGE

BMDCs were left untreated or were incubated with OVA IC for 24 hours and 48 hours. Residual immune complexes were removed by washing with culture medium. Subsequently, cells were incubated with 1 μM quenched activity-based probe BMV109 for 1 hour at 37°C. After washing with PBS total cell lysates were prepared and proteins were separated by SDS-PAGE (200.000 cells/lane) on a 15% polyacrylamide gel. Cy5 labeled cathepsins were measured directly in the gel with the Typhoon Imager.

ACKNOWLEDGEMENTS

This work was financially supported by ZonMW TOP 91211011 to Nataschja I Ho. N.I.H., M.G.M.C., F.O. designed the study. N.I.H., M.G.M.C., J.J.G.V., E.B., carried out research experiments. N.I.H., M.G.M.C., J.J.G.V., E.B., F.O. analysed the data. N.I.H. and F.O. wrote the paper. M.V., Y.v.K. read the manuscript.

REFERENCES

1. Fehres, C. M., W. W. J. Unger, J. J. Garcia-Vallejo, and Y. van Kooyk. Understanding the Biology of Antigen Cross-Presentation for the Design of Vaccines Against Cancer. *Front. Immunol.* 2014. 5: 149.
2. Embgenbroich, M., and S. Burgdorf. Current Concepts of Antigen Cross-Presentation. *Front. Immunol.* 2018. 9: 1643.
3. Ho, N. I., L. G. M. Huis in 't Veld, T. K. Raaijmakers, and G. J. Adema. Adjuvants Enhancing Cross-Presentation by Dendritic Cells: The Key to More Effective Vaccines? *Front. Immunol.* 2018. 9: 2874.
4. Shen, L., L. J. Sigal, M. Boes, and K. L. Rock. Important role of cathepsin S in generating peptides for TAP-independent MHC class I crosspresentation in vivo. *Immunity* 2004. 21: 155–165.
5. Kovacsovics-Bankowski, M., and K. L. Rock. A phagosome-to-cytosol pathway for exogenous antigens presented on MHC class I molecules. *Science* 1995. 267: 243–246.
6. Ackerman, A. L., C. Kyritsis, R. Tampe, and P. Cresswell. Early phagosomes in dendritic cells form a cellular compartment sufficient for cross presentation of exogenous antigens. *Proc. Natl. Acad. Sci.* 2003. 100: 12889–12894.
7. Palmowski, M. J., U. Gileadi, M. Salio, A. Gallimore, M. Millrain, E. James, C. Addey, D. Scott, J. Dyson, E. Simpson, and V. Cerundolo. Role of Immunoproteasomes in Cross-Presentation. *J. Immunol.* 2006. 177: 983–990.
8. Saveanu, L., O. Carroll, M. Weimershaus, P. Guermonprez, E. Firat, V. Lindo, F. Greer, J. Davoust, R. Kratzer, S. R. Keller, G. Niedermann, and P. van Endert. IRAP Identifies an Endosomal Compartment Required for MHC Class I Cross-Presentation. *Science* 2009. 325: 213–217.
9. Van Montfoort, N., M. G. Camps, S. Khan, D. V. Filippov, J. J. Weterings, J. M. Griffith, H. J. Geuze, T. van Hall, J. S. Verbeek, C. J. Melief, and F. Ossendorp. Antigen storage compartments in mature dendritic cells facilitate prolonged cytotoxic T lymphocyte cross-priming capacity. *Proc. Natl. Acad. Sci. U. S. A.* 2009. 106: 6730–6735.
10. Henrickson, S. E., T. R. Mempel, I. B. Mazo, B. Liu, M. N. Artyomov, H. Zheng, A. Peixoto, M. P. Flynn, B. Senman, T. Junt, H. C. Wong, A. K. Chakraborty, and U. H. von Andrian. T cell sensing of antigen dose governs interactive behavior with dendritic cells and sets a threshold for T cell activation. *Nat. Immunol.* 2008. 9: 282–291.
11. Ossendorp, F., N. Fu, M. Camps, F. Granucci, S. J. P. Gobin, P. J. van den Elsen, D. Schuurhuis, G. J. Adema, G. B. Lipford, T. Chiba, A. Sijts, P.-M. Kloetzel, P. Ricciardi-Castagnoli, and C. J. M. Melief. Differential Expression Regulation of the α and β Subunits of the PA28 Proteasome Activator in Mature Dendritic Cells. *J. Immunol.* 2005. 174: 7815–7822.
12. Verdoes, M., K. Oresic Bender, E. Segal, W. A. van der Linden, S. Syed, N. P. Withana, L. E. Sanman, and M. Bogyo. Improved quenched fluorescent probe for imaging of cysteine cathepsin activity. *J. Am. Chem. Soc.* 2013. 135: 14726–14730.
13. Streng-Ouwehand, I., N. I. Ho, M. Litjens, H. Kalay, M. A. Boks, L. A. M. Cornelissen, S. K. Singh, E. Saeland, J. J. Garcia-Vallejo, F. A. Ossendorp, W. W. J. Unger, and Y. van Kooyk. Glycan modification of antigen alters its intracellular routing in dendritic cells, promoting priming of T cells. *Elife* 2016. 5: pii: e11765.
14. Nakagawa, T. Y., W. H. Brissette, P. D. Lira, R. J. Griffiths, N. Petrushova, J. Stock, J. D. McNeish, S. E. Eastman, E. D. Howard, S. R. Clarke, E. F. Rosloniec, E. A. Elliott, and A. Y. Rudensky. Impaired invariant chain degradation and antigen presentation and diminished collagen-induced arthritis in cathepsin S null mice. *Immunity* 1999. 10: 207–217.
15. Shi, G. P., J. A. Villadangos, G. Dranoff, C. Small, L. Gu, K. J. Haley, R. Riese, H. L. Ploegh, and H. A. Chapman. Cathepsin S required for normal MHC class II peptide loading and germinal center development. *Immunity* 1999. 10: 197–206.
16. Lautwein, A., T. Burster, A.-M. Lennon-Duménil AM, H. S. Overkleeft, E. Weber, H. Kalbacher, C. Driessen, A.-M. Lennon-Duménil, H. S. Overkleeft, E. Weber, H. Kalbacher, and C. Driessen. Inflammatory stimuli recruit cathepsin activity to late endosomal compartments in human dendritic cells. *Eur. J. Immunol.* 2002. 32: 3348–3357.
17. Delamarre, L., M. Pack, H. Chang, I. Mellman, and E. S. Trombetta. Differential Lysosomal Proteolysis in Antigen-Presenting Cells Determines Antigen Fate. *Science* 2005. 307: 1630–1634.
18. Perišić Nanut, M., J. Sabotič, A. Jewett, and J. Kos. Cysteine cathepsins as regulators of the cytotoxicity of NK and T cells. *Front. Immunol.* 2014. 5: 616.

19. Kos, J., Z. Jevnikar, and N. Obermajer. The role of cathepsin X in cell signaling. *Cell Adh. Migr.* 2009. 3: 164–166.
20. Obermajer, N., U. Svajger, M. Bogyo, M. Jeras, and J. Kos. Maturation of dendritic cells depends on proteolytic cleavage by cathepsin X. *J. Leukoc. Biol.* 2008. 84: 1306–1315.
21. Nair-Gupta, P., A. Baccarini, N. Tung, F. Seyffer, O. Florey, Y. Huang, M. Banerjee, M. Overholtzer, P. A. Roche, R. Tampé, B. D. Brown, D. Amsen, S. W. Whiteheart, and J. M. Blander. TLR signals induce phagosomal MHC-I delivery from the endosomal recycling compartment to allow cross-presentation. *Cell* 2014. 158: 506–521.
22. Ho, N. I., M. G. M. Camps, E. F. E. de Haas, and F. Ossendorp. Sustained cross-presentation capacity of murine splenic dendritic cell subsets in vivo. *Eur. J. Immunol.* 2018. 48: 1164–1173.
23. Allan, R. S., J. Waithman, S. Bedoui, C. M. Jones, J. A. Villadangos, Y. Zhan, A. M. Lew, K. Shortman, W. R. Heath, and F. R. Carbone. Migratory Dendritic Cells Transfer Antigen to a Lymph Node-Resident Dendritic Cell Population for Efficient CTL Priming. *Immunity* 2006. 25: 153–162.
24. Srivastava, S., and J. D. Ernst. Cell-to-cell transfer of M. tuberculosis antigens optimizes CD4 T cell priming. *Cell Host Microbe* 2014. 15: 741–752.
25. Gurevich, I., T. Feferman, I. Milo, O. Tal, O. Golani, I. Drexler, and G. Shakhar. Active dissemination of cellular antigens by DCs facilitates CD8+ T-cell priming in lymph nodes. *Eur. J. Immunol.* 2017. 47: 1802–1818.
26. Eickhoff, S., A. Brewitz, M. Y. Gerner, F. Klauschen, K. Komander, H. Hemmi, N. Garbi, T. Kaisho, R. N. Germain, and W. Kastenmüller. Robust Anti-viral Immunity Requires Multiple Distinct T Cell-Dendritic Cell Interactions. *Cell* 2015. 162: 1322–1337.
27. Hor, J. L., P. G. Whitney, A. Zaid, A. G. Brooks, W. R. Heath, and S. N. Mueller. Spatiotemporally Distinct Interactions with Dendritic Cell Subsets Facilitates CD4+ and CD8+ T Cell Activation to Localized Viral Infection. *Immunity* 2015. 43: 554–565.
28. Kitano, M., C. Yamazaki, A. Takumi, T. Ikeno, H. Hemmi, N. Takahashi, K. Shimizu, S. E. Fraser, K. Hoshino, T. Kaisho, and T. Okada. Imaging of the cross-presenting dendritic cell subsets in the skin-draining lymph node. *Proc. Natl. Acad. Sci. U. S. A.* 2016. 113: 1044–1049.
29. Borst, J., T. Ahrends, N. Bąbała, C. J. M. Melief, and W. Kastenmüller. CD4+ T cell help in cancer immunology and immunotherapy. *Nat. Rev. Immunol.* 2018. 18: 635–647.
30. Bachem, A., S. Güttler, E. Hartung, F. Ebstein, M. Schaefer, A. Tannert, A. Salama, K. Movassaghi, C. Opitz, H. W. Mages, V. Henn, P.-M. Kloetzel, S. Gurka, and R. A. Kroczek. Superior antigen cross-presentation and XCR1 expression define human CD11c+CD141+ cells as homologues of mouse CD8+ dendritic cells. *J. Exp. Med.* 2010. 207: 1273–1281.
31. Brewitz, A., S. Eickhoff, S. Dähling, T. Quast, S. Bedoui, R. A. Kroczek, C. Kurts, N. Garbi, W. Barchet, M. Iannacone, F. Klauschen, W. Kolanus, T. Kaisho, M. Colonna, R. N. Germain, and W. Kastenmüller. CD8 + T Cells Orchestrate pDC-XCR1 + Dendritic Cell Spatial and Functional Cooperativity to Optimize Priming. *Immunity* 2017. 46: 205–219.
32. Peters, P. J., E. Bos, and A. Griekspoor. Cryo-immunogold electron microscopy. *Curr. Protoc. cell Biol.* 2006. Chapter 4: Unit 4.7.

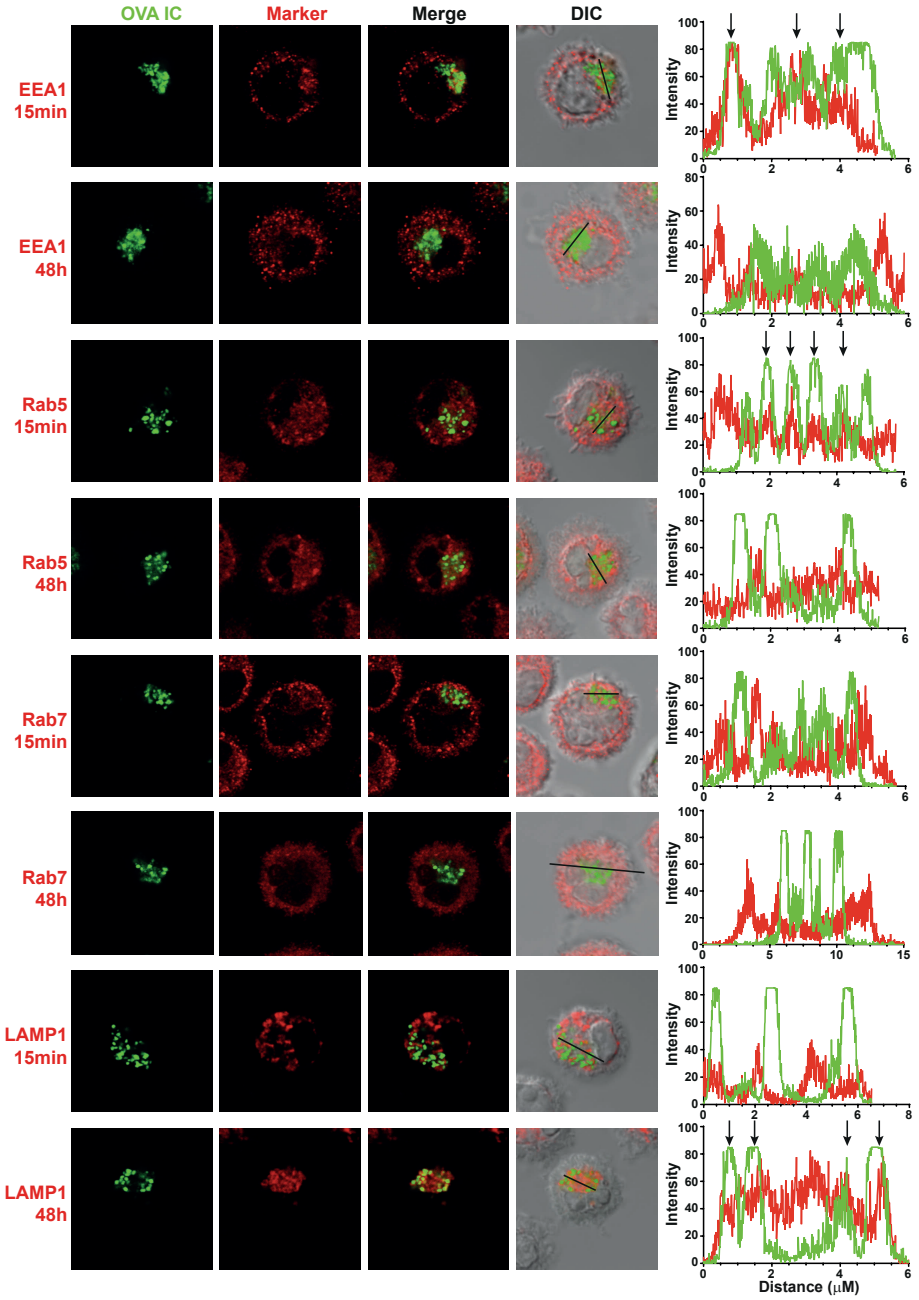

Supplemental Figure 1. Characterization of the antigen storage compartments in DCs upon FcγR targeting. DCs were pulsed with OVA IC (Alexa Fluor 488, green) for 15 min or pulsed with OVA IC for 2 hours and chased for 48 hours. OVA IC presence in DCs was imaged by confocal microscopy and DIC was used to image cell contrast. Specific antibodies against EEA1, Rab5, Rab7, LAMP1, MHCI, MHCII, TAP1, and PA28β (red) were used and analyzed for co-localization with OVA IC (green). Histograms for each fluorophore were created for a selected area (indicated by a line on the image) and overlays were made with the ImageJ software. Arrows indicate co-localization between OVA IC (green) and the specific antibody (red).

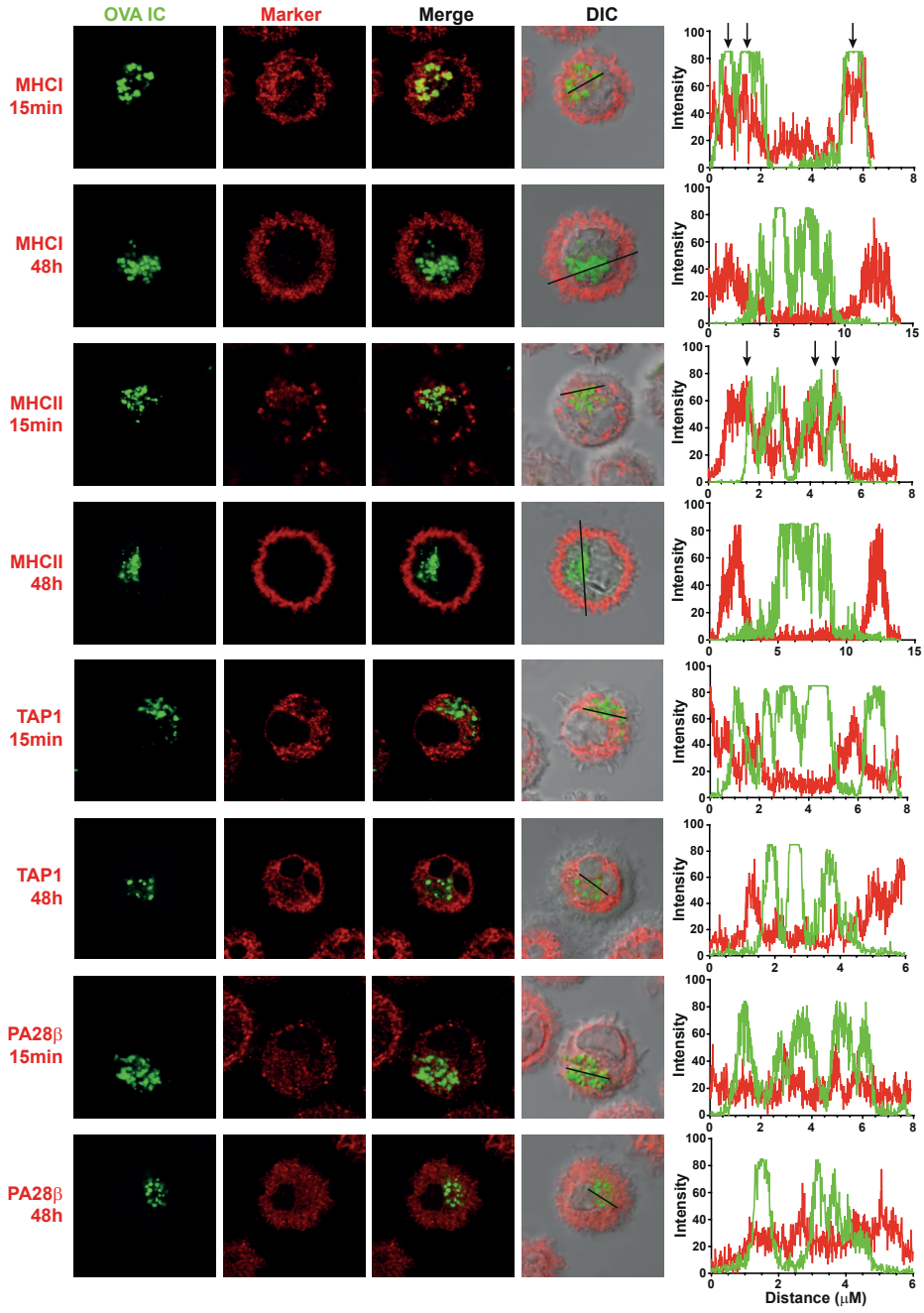

Supplemental Figure 1. Continued.

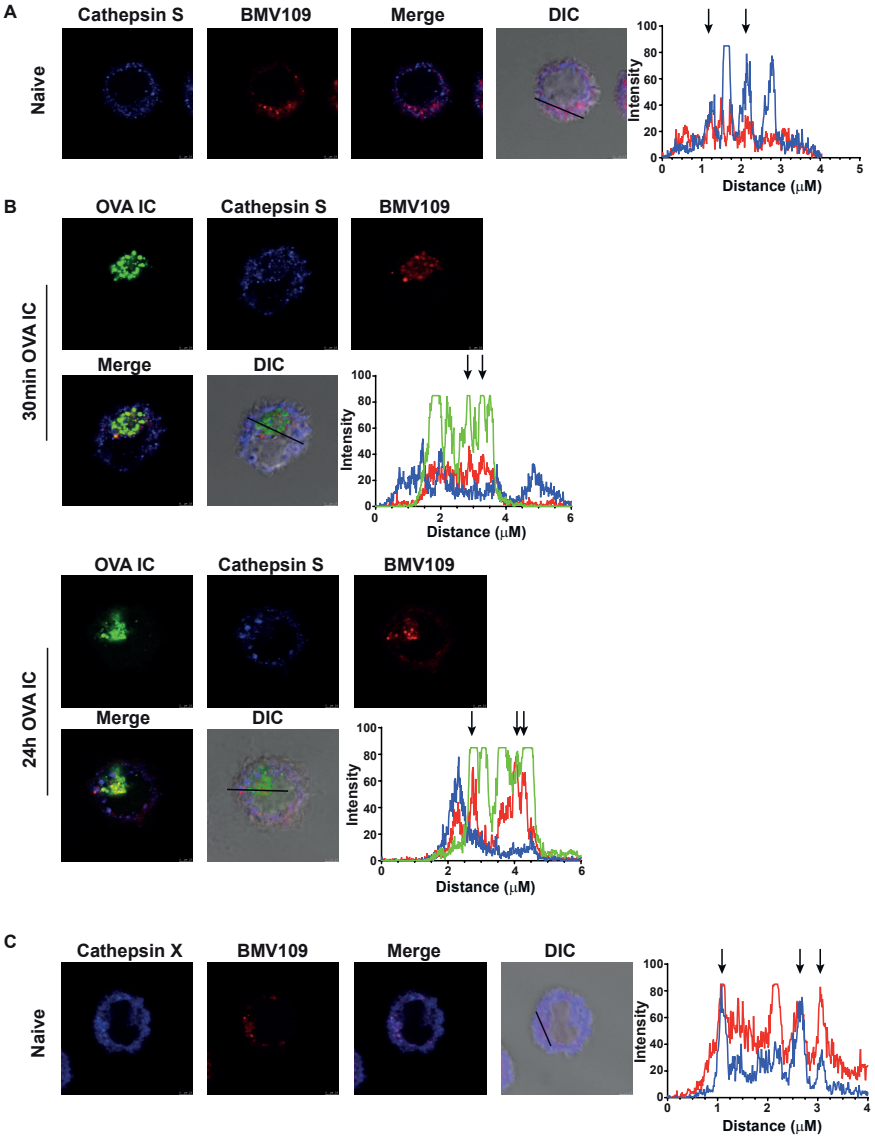

Supplemental Figure 2. The presence of cathepsins in the antigen storage compartments in DCs. Co-localization between quenched activity-based probe BMV109 and specific antibody against cathepsin S was analyzed in naïve DCs with confocal microscopy and DIC was used to image cell contrast. Histograms for each fluorophore were created for a selected area (indicated by a line on the image) and overlays were made with the ImageJ software. Arrows indicate co-localization between cathepsin S (blue) and BMV109 (red) **(A)**. DCs were pulsed with OVA IC (Alexa Fluor 488) for 30 min or pulsed for 2 hours and chased for 24 hours. Co-localization between OVA IC (green), cathepsin S (blue), BMV109 (red) was analyzed by confocal microscopy and indicated by arrows **(B)**. Co-localization between BMV109 and specific antibody against cathepsin X was analyzed in naïve DCs with confocal microscopy. Arrows indicate co-localization between cathepsin X (blue) and BMV109 (red) **(C)**. DCs pulsed with OVA IC (Alexa Fluor 488) for 30 min, 1, 2, 3 hours or DCs pulsed for 2 hours and chased for 24 hours were stained for cathepsin X or BMV109. Co-localization between OVA IC (green), cathepsin X (blue) or BMV109 (red) was analyzed by confocal microscopy and indicated by arrows **(D)**.

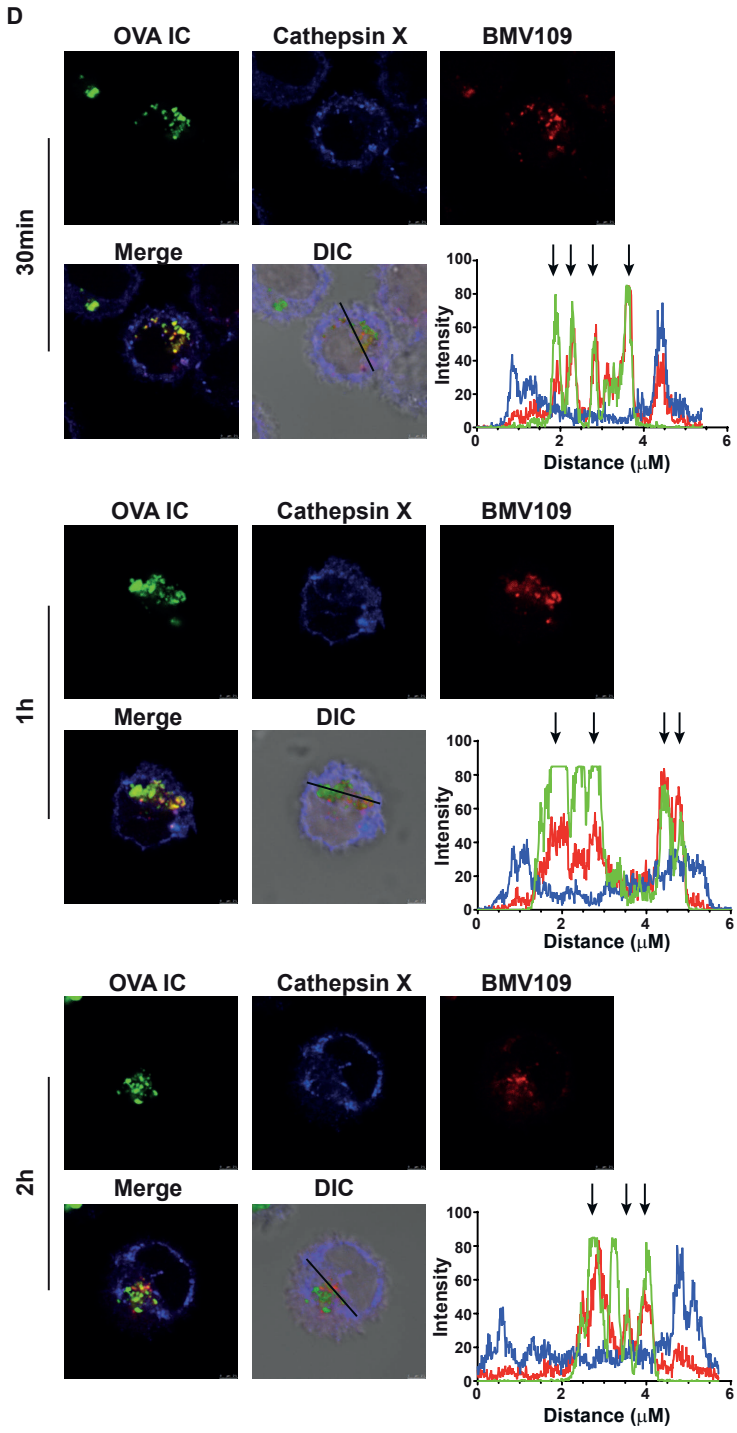

Supplemental Figure 2. Continued.

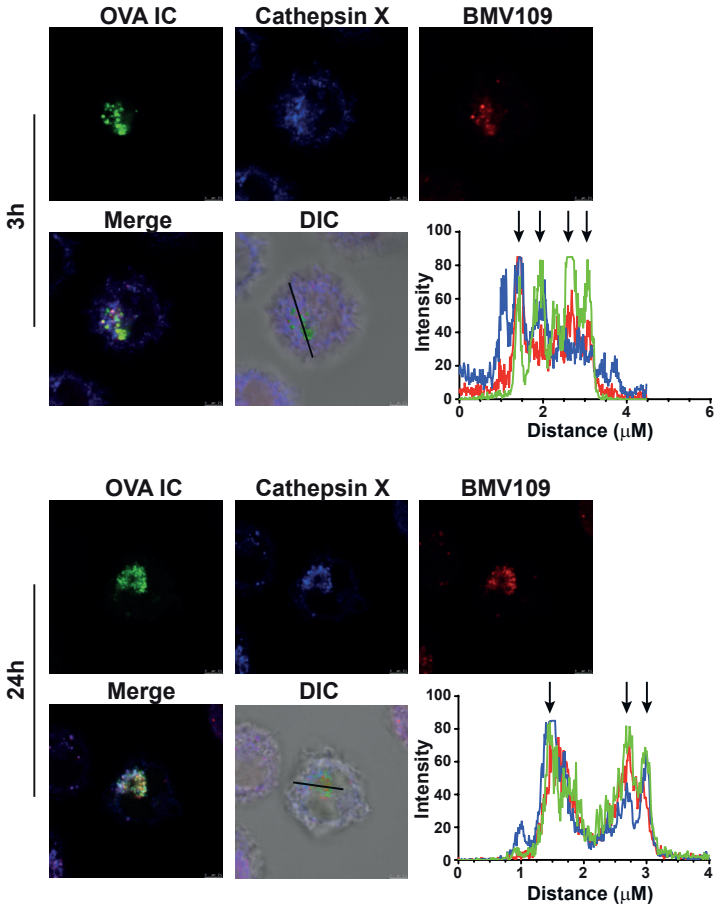

Supplemental Figure 2. Continued.

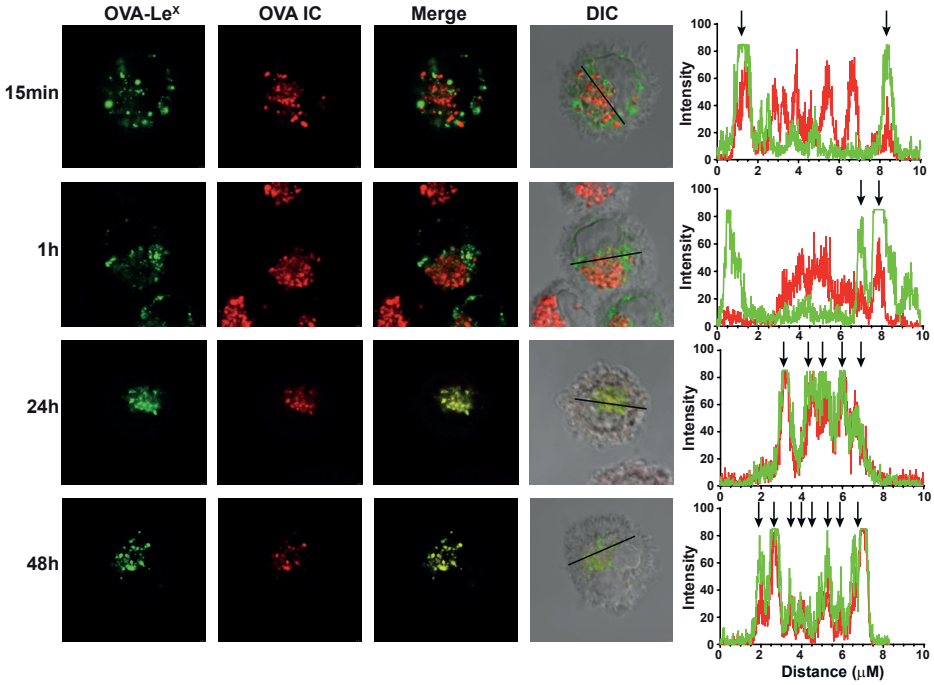

Supplemental Figure 3. Antigens targeted to FcγRs and MGL1 on DCs end up in the same compartment. DCs were pulsed with OVA IC (Alexa Fluor 647) or OVA-Le^x (Dylight 488) for 15 min and 1 hour, or pulsed for 2 hours and chased for 24 or 48 hours. Co-localization between OVA IC and OVA-Le^x was visualized by confocal microscopy and DIC was used to image cell contrast. Histograms for each fluorophore were created for a selected area (indicated by a line on the image) and overlays were made with the ImageJ software. Arrows indicate co-localization between OVA IC (red) and OVA-Le^x (green).

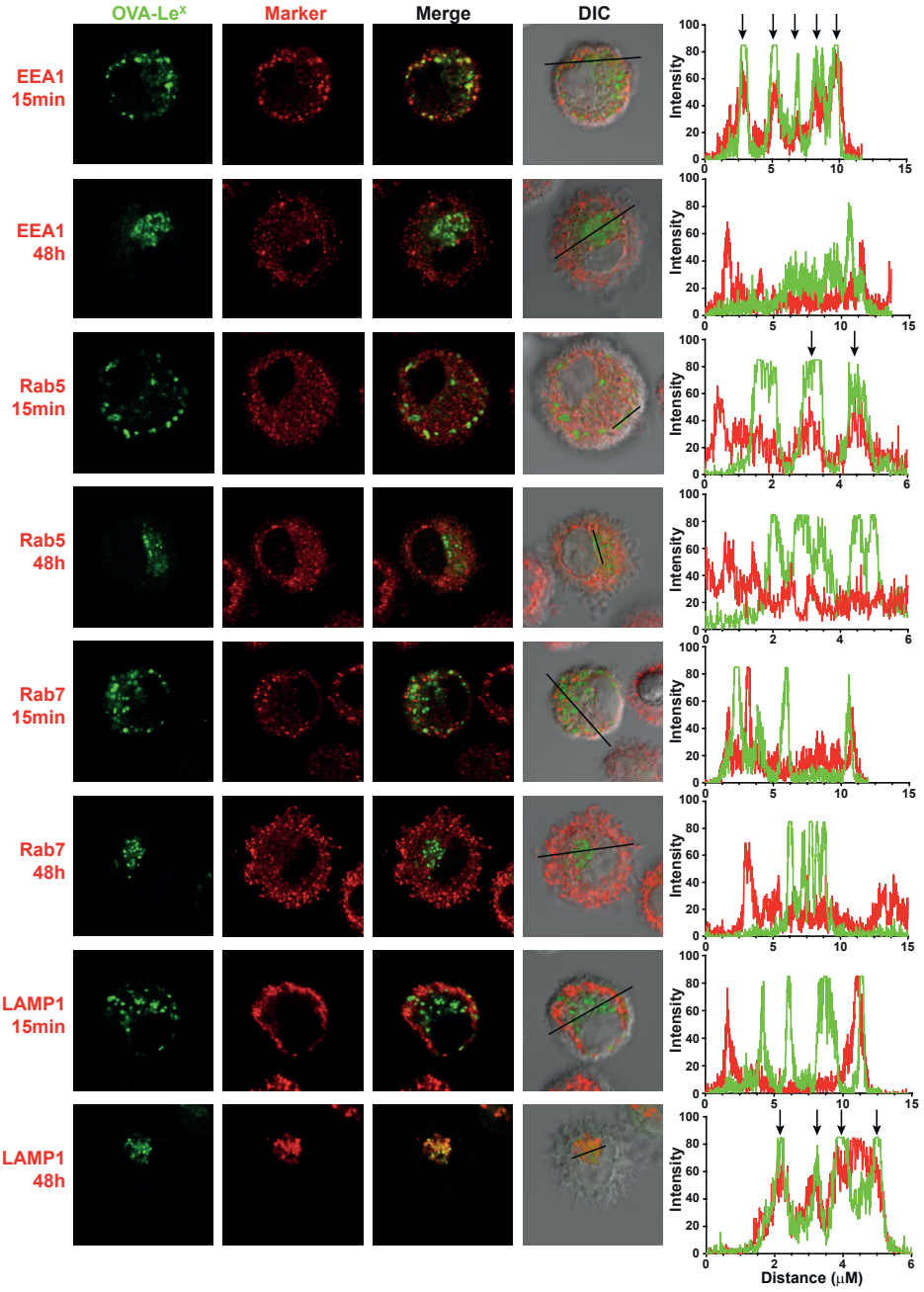

Supplemental Figure 4. Characterization of the antigen storage compartments in DCs upon MGL1 targeting. DCs were pulsed with OVA-Le^x (Dylight 488) for 15 min or pulsed with OVA-Le^x for 2 hours and chased for 48 hours. OVA-Le^x presence in DCs was imaged by confocal microscopy and DIC was used to image cell contrast. Specific antibodies against EEA1, Rab5, Rab7, LAMP1, MHCI, MHCII, TAP1, and PA28β (red) were used and analyzed for co-localization with OVA-Le^x (green). Histograms for each fluorophore were created for a selected area (indicated by a line on the image) and overlays were made with the ImageJ software. Arrows indicate co-localization between OVA-Le^x (green) and the specific antibody (red).

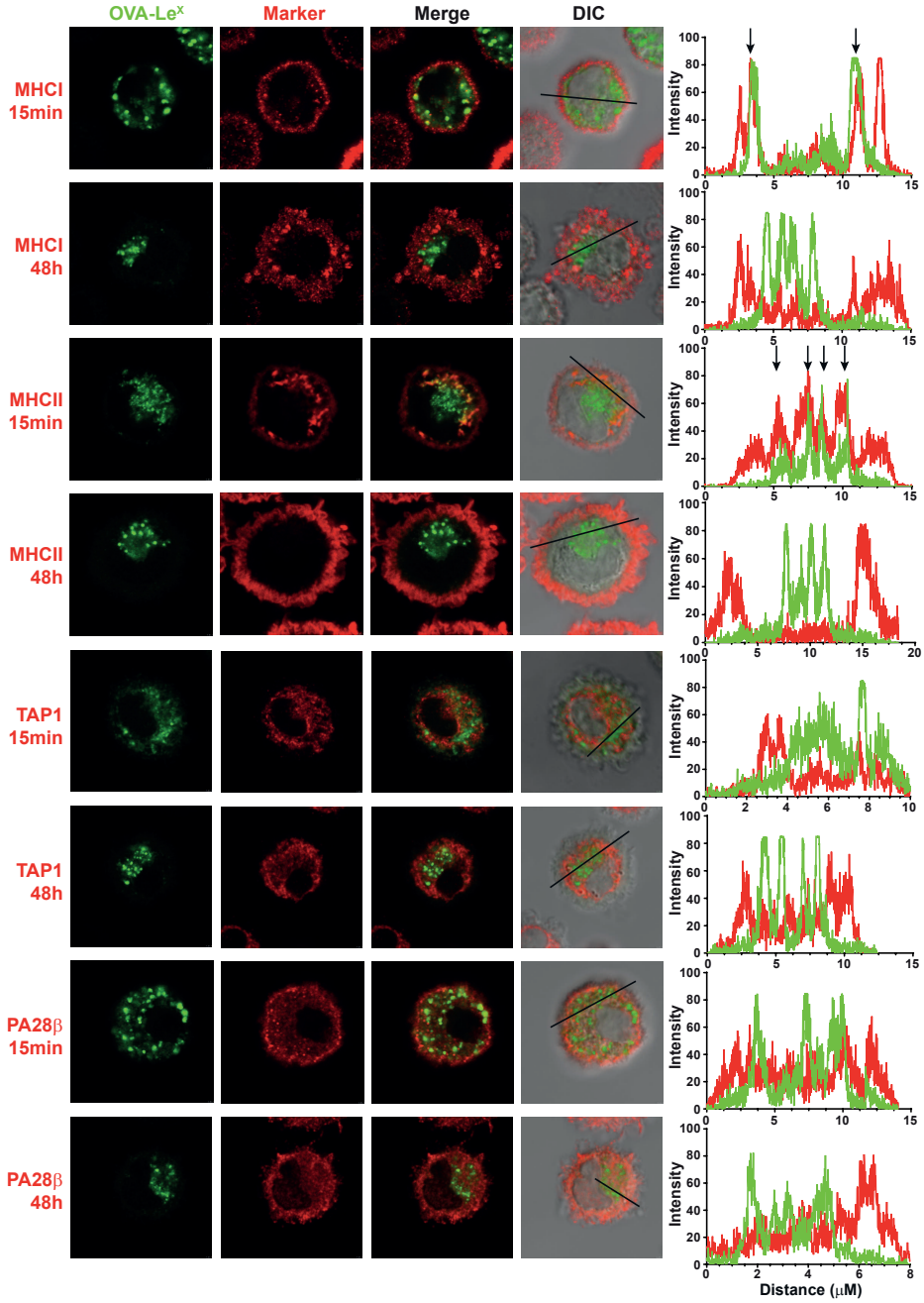

Supplemental Figure 4. Continued.